Proceedings World Geothermal Congress 2015
Melbourne, Australia, 19-25 April 2015

Comparison of 1-D, 2-D and 3-D Inversion Approaches of Interpreting Electromagnetic Data of Silali Geothermal Area

Charles Muturia Lichoro

Geothermal Development Company Ltd, P. O. Box 1770 Nakuru, 20100

E-mail: cmuturia@gdc.co.ke

Keywords: Geothermal, Magnetotelluric, Transient Electromagnetic, Inversions, Silali, Kenya

ABSTRACT

With development of MT interpretation codes and advancement in computer hardware, 3-D electromagnetic data interpretation has become attainable. This study therefore seeks to compare results of Electromagnetic data using different interpretational techniques in order to provide reliable information about the presence, location, and size of geothermal systems in Silali field. Resistivity study of the Silali area in Kenya was carried out by the combined use of TEM and MT soundings. Joint inversion of the EM data was used to correct for static shifts in the MT data, which can be severe due to large near-surface resistivity contrasts. Joint 1-D inversion of 102 TEM/MT sounding pairs and a 3-D inversion of a 97 sounding subset of the MT data were performed. Additionally 2-D inversion of the same data set was done and results are compared with those of 1-D and 3-D inversion models. The resistivity models resulting from the 3-D inversion were elevation corrected and smoothed and are presented as planar maps and cross sections. The inverted model of electrical resistivity reveals the presence of highly resistive near surface layer, identified as unaltered formations, which covers a low resistivity cap corresponding to the smectite-zeolite zone. Beneath this cap a more resistive zone is identified as the epidote-chlorite zone (the resistive core) and interpreted as the host of geothermal reservoir. Further at depth of about 6 km an electrically conductive feature has been imaged, and has been tentatively interpreted as a heat source for geothermal system in this field.

The aim of modelling EM data using all the three interpretational techniques is to compare results and establish which resistivity anomalies stand out irrespective of the dimensional inversion used. In this study results from 1-D, 2-D and 3-D models recover near surface resistivity structure fairly well but differ somewhat at depth. The 3-D inversion however reveals much more consistent details than the 1-D and 2-D inversion confirming that the resistivity structures in the area are highly three dimensional. At depth below 6 km the three approaches give different results implying that the models do not resolve deeper structures. This has been attributed to noise in the data at long periods.

1. INTRODUCTION

The electromagnetic methods that include magnetotelluric (MT) and transient electromagnetic (TEM) are techniques of choice when it comes to geothermal exploration. This is because they give indirect information about the sub-surface, in terms of the resistivity structure of geothermal systems that may be connected to temperature and other components that are of interest. A total of 102 MT soundings and an equal number of TEM soundings are used in the interpretation. This report describes a multi-dimensional inversion of static shift corrected MT data set from Silali area.

The MT method suffers from the static shift problem. This is an inherent uncertainty in the MT data, caused mainly by local near-surface resistivity heterogeneities close to the sounding site (Sternberg et al., 1988; Árnason, 2008). This phenomenon cannot be resolved using MT data alone. The static shift is expressed by scaling of the apparent resistivity by an unknown factor (shifted on log scale), so that apparent resistivity curves plot parallel to their true level. This may lead to very wrong and misleading interpretation of MT data if the static shift is not corrected. The TEM method does not suffer this problem, therefore joint inversion of TEM and MT soundings done at the same location has been used to determine and correct for the static shift in the MT data.

Joint 1-D inversion of MT and TEM recovers resistivity variation only with depth, from which models have been stitched together to produce spatial resistivity variation and cross-sections in the area of interest. 2-D inversion models present resistivity cross-sections where resistivity is assumed to vary with depth and in one horizontal direction, but being constant in the other orthogonal horizontal direction. Data has been interpreted by use of TE, TM and combined TE+TM modes with the aim of evaluating which of the modes recovers the resistivity structure more accurately. TE-mode describes current flowing parallel to strike whereas TM-mode describes current crossing the structure. Recent developments of inversion codes and computer hardware (computer clusters) have made 3-D inversion of MT data practical. The real Earth is 3-dimensional where conductivity varies in all directions, $\sigma(x, y, z)$. In this regard the 3-D MT inversion of the off-diagonal impedance tensor has been performed resulting in much more reliable and detailed results than previously attained. The results are compared with the results of the joint 1-D inversion of the TEM and MT data and those of the 2-D inversion models.

2. LOCATION OF SILALI GEOTHERMAL AREA

The Silali volcanic system is located within the East African rift system (EARS) consisting of a central volcano with a caldera aligned in NW-SE direction and fissures and faults trending in NNE-SSW. This area has experienced immense volcanism and faulting which has motivated investigation of its geothermal potential. Kenya's Geothermal Development Company (GDC) has explored for geothermal resource in this prospect and is in the process of initiating development soon. Extensive geophysical surveys including resistivity (TEM and MT) have been done to delineate the geothermal anomaly. This study seeks to examine the resistivity distribution within the Silali volcanic region in order to define the magmatic, geothermal, and structural features of this active volcano. Recent fissure eruptions occurred about 200-300 years ago in the eastern sector of the Silali volcano. At volcanoes

where there has been recent eruption activity, like Silali caldera, magma remnants at depth can be imaged using resistivity investigation.

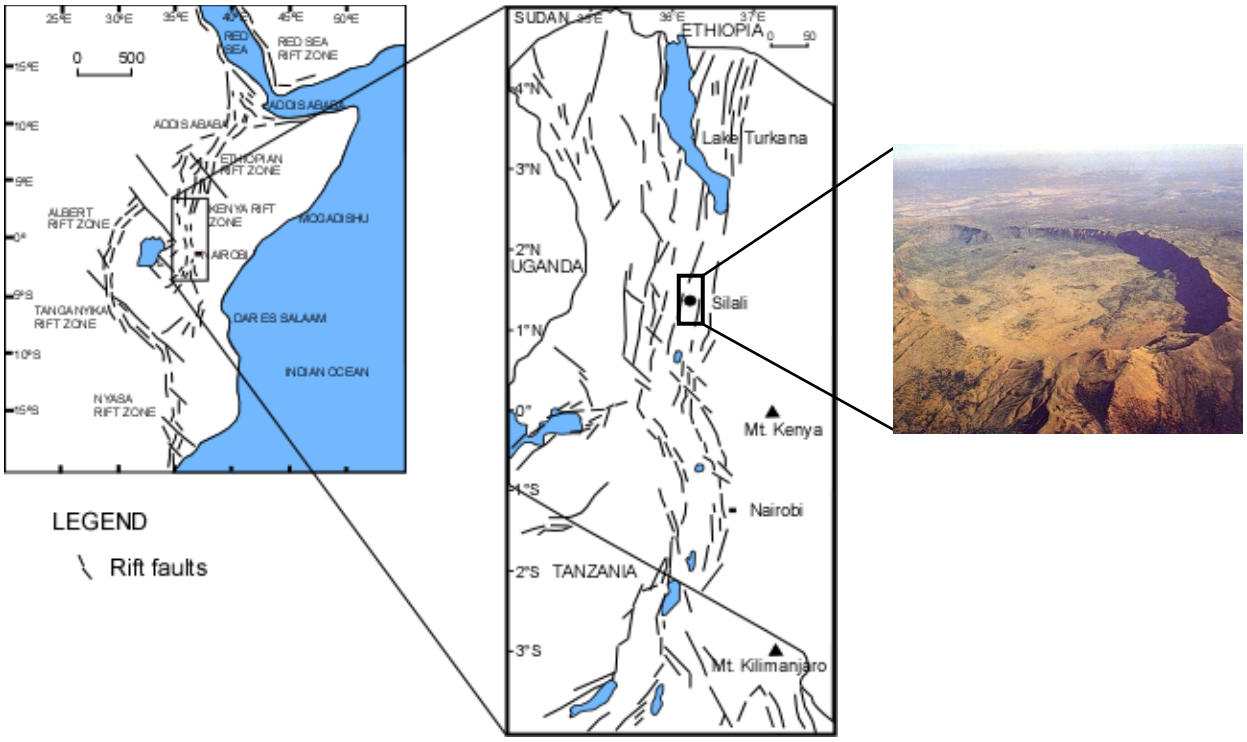

Figure1: Map showing the Kenya Rift and the volcanic centers and lakes. Silali (rectangular box) is the volcanic centre of focus for this study.

3. JOINT 1-D INVERSION OF TEM AND MT SOUNDINGS

The one-dimensional joint inversion is performed simultaneously for both TEM and MT data by fitting both data sets to obtain one model. This is achieved by use of an algorithm which determines the appropriate shift factor to be used to constrain the MT data to fit the TEM response. Both the MT and TEM data collected on approximately the same location are brought together in a joint inversion which also determines a static shift multiplier to correct for static shift that is inherent in MT data.

Joint 1-D Occam inversion has been done for the rotationally invariant determinant apparent resistivity and phase of all the MT soundings and their nearest TEM soundings in the Silali field. Determinant data is preferred because it is rotationally invariant and averages out all "dimensionality" of data. It is unique and independent of the strike direction. An example of a 1-D joint inversion of MT and TEM data is shown on Figure 2. The shift multiplier is shown in the upper right hand corner of the apparent resistivity panel. The best fit for this pair was achieved with a shift parameter of S = 0.716. This means that the MT apparent resistivity has to be divided by this value to be consistent with the associated TEM sounding.

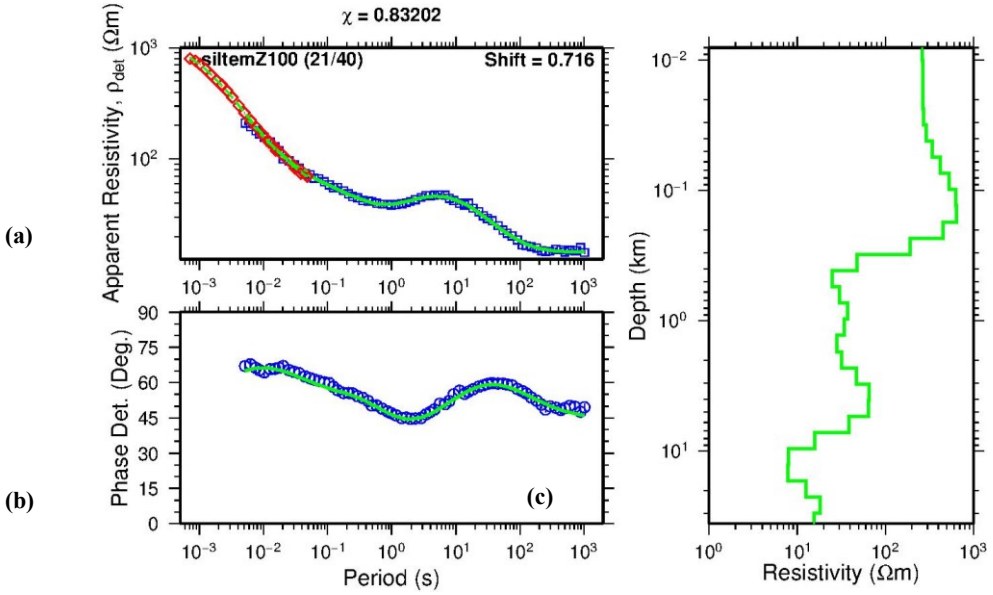

Figure 2: Typical result of a joint 1-D inversion of TEM and MT soundings; where the red diamonds in Figure 1a are measured TEM apparent resistivities and blue squares are the MT apparent resistivities and phase Figure 2a and 2b). Solid lines show the response of the resistivity model on Figure 2c. The shift multiplier is shown in the upper right hand corner of the apparent resistivity panel Figure 2a.

3.1 Joint inversion 1-D Results

3.1.1 1-D Cross-sections

Resistivity cross-sections are plotted for results obtained from 1-D inversion by a program called TEMCROSS (Eysteinsson, 1998), developed at Iceland Geosurvey. The program calculates the best line between selected soundings on a profile, and plots resistivity isolines based on the 1-D model for each sounding. It is actually the logarithm of the resistivity that is contoured so the colour scale is exponential but numbers at contour lines are actual resistivity values. Cross-sections were made through the survey area and profiles were positioned perpendicular to the inferred geoelectrical strike direction (N10°E). Cross-sectional maps are shown in Figures 4a and 5a).

3.1.2 1-D Iso-resistivity maps

Iso-resistivity maps are made by a program known as TEMRESD which generates iso-resistivity maps at fixed elevations derived from the 1-D Occam models (Eysteinsson, 1998). The resistivity is contoured and coloured in a logarithmic scale. The general elevation of the Silali volcano is about 1000 - 1200 m a.s.l. The maps show that resistivity varies considerably both laterally and with depth (see maps in Figure 6a and 7a).

3.1.3 Discussion of 1-D inversion results

Joint inversion of TEM and rotationally invariant determinant MT data reveals a resistivity structure consisting generally of a shallow low-resistivity layer particularly around the caldera, in the uppermost 1 km, underlain by high resistivity. At greater depth, a second conductive layer is observed in the northeast, southeast and in the west of the caldera. The upper low-resistivity layer presumably reflects conductive hydrothermal alteration minerals formed at temperatures between 100 and 240 °C. The resistive core reflects the change in alteration to resistive high temperature minerals which could be hosting the geothermal system in Silali field. The nature of the deep conductive layer is not as clear in absence of other geophysical data, but could be attributed to magmatic heat sources.

4. 2-D INVERSION OF MT DATA

The inversions of MT data was performed by use of REBOCC program along profiles running perpendicular to the regional strike. The program finds a minimum structure model subject to a desired misfit level. The starting model used in the 2-D inversion was a 10 Ωm homogeneous half-space, and the iterations were set to 10 with RMS misfit of 1. It should be noted that the desired RMS achieved in all profiles was in the range between 5 to 11, this was as a result of the model responses not fitting well to the data which imply that the data was not fully 2-dimensional. For each profile two data responses and their corresponding error responses for both apparent resistivity and phase were generated each for TE and TM-mode and used as input to REBOCC. A total of 73 periods ranging from 0.0031 to 877 seconds were included in the data file for each profile. Several half-space initial models were used to check model convergence and fitting to the data and 10 Ωm homogeneous half-space was found to be the best. REBOCC is very fast and converges to a reliable inversion with minimal memory usage.

4.1 2-D inversion Results

This section describes results from two profiles running perpendicular to the strike direction. Each of the profiles present three cross-sections for TE-mode, TM-mode and a combined TE+TM-mode. Two-dimensional models usually have anisotropic responses. For instance inverting each mode separately yields two different resistivity structures. This difference in modes is due to different sensitivity to complex structures and does not always imply anisotropy.

4.2 Discussion of 2-D inversion results

2-D inversion were carried out to define subsurface conductive structures but a single model that explains both TE and TM models may not exist. The TM-model provides better resolution of higher resistive blocks, which can be explained in terms of boundary conditions. The electric field in the TM-mode is perpendicular to strike and thus, discontinuous across lateral changes in resistivities. In this case the TM-mode is more robust for the presence of 3-D structures (Wannamaker et al.,1991).

The main result from inversion of profiles presented in Figure 4b and 5b can be summarized as follows: four main resistivity layers are revealed from the 2-D inversion. These are a thin surface layer of high resistivity (≥ 100 Ωm) followed by conductive layer of about 10 Ωm, underlain by a high resistivity core of about 100 Ωm and a deep low resistivity of ≤ 10 Ωm. The surface high-resistivity layer can be correlated to unaltered basaltic lava flows and other eruptive materials. The second layer is very conductive and can be associated with altered formations and clays (smectite-zeolite or mixed layer clay alteration zone). The high resistivity core below the conductive layer can be correlated to chlorite-epidote alteration zone down to a depth of about 3 km. This high-resistivity zone below the conductive layer could be related to the reservoir of the geothermal system. At depth of 5-6 km a deeper conductor appears on mainly the TM and TE+TM-mode cross-sections. This deeper conductive structure, if real, could be the heat source of the geothermal system. Although the results of the inversion model seems to reproduce main structures, the poor fit of the model responses to the some data would not guarantee enough confidence in the inversion model obtained. 2-D inversions are known to introduce spurious features in the interpretation when they cannot resolve the features due to off-profile 3-D structures (Siripunvaraporn et al., 2005). Moreover, the resistivity distribution of real geological structures is often very complex and does not satisfy the 2-D assumption. Therefore to solve this problem, 3-D MT inversion of the MT data is essential.

5. 3-D INVERSION OF MT DATA

With the development of MT interpretation codes and advances in computer hardware 3-D electromagnetic data interpretation has become attainable. Dimensionality analysis of the MT data from Silali field show non one-dimensional resistivity structure mainly at long periods. It is therefore necessary to carry out 3-D inversion to determine the correct resistivity structure. This is achieved by use of a 3-D inversion program, WSINV3-DMT version 1.1.0 (Siripunvaraporn et al., 2005) which seeks to find a model with a response that fits the data. This inversion code uses finite difference forward algorithm and formulates the inversion problem in data-space rather than the more computationally demanding model-space approach. Therefore this scheme significantly reduces the computational time and memory required for the inversion making the 3-D inversion of MT data possible.

5.1 Data preparation

The modelling data used for the 3-D inversion are: 97 MT soundings, 30 periods and 4 impedance tensor elements. The MT soundings chosen were those that were less noisy and with long period data points and evenly distributed over the entire area. All the MT impedances were rotated to N10°E which is the strike direction. In order to minimize the computational time and memory the impedance data was sampled at 30 periods equally spaced on a log scale, ranging from 0.0031 to 700 seconds. This not only reduces the data size but also makes the data to be more smoother. If there are any noisy data points in the resampled data set a skipfile is prepared to be used during inversion to skip those noisy data points so that they were not included in the inversion.

5.2 3-D Model mesh grid design

When setting up a 3-D model grid, it must be ensured that it is accurate for the resistivities and frequencies to be used. In designing the mesh a trade-off is sought between the size of the grid and the computational time it would require to obtain reasonable solutions to the models. This is because the finer the grid the larger the time and memory resource required. Forward modelling solutions depend significantly on the mesh grid discretization used. The finite difference code for the forward problem requires a cubic grid, in this case a grid of 73 x 86 x 28 in x, y, and z directions was used. This gave a total model size M to be equal to 73 × 86 × 28 = 175,784. At the centre of the grid a uniform model discretization with a cell width of 350 m for 49 x 62 grid squares in x and y directions was used within the area containing MT stations. This grid increases exponentially in size to 139.4 km and 141.8 km in the x and y directions respectively. In the z direction the grid planes are dense at shallow depth with the first layer set at 16 m and then increased progressively by 1.4 times of the overlying block to depths of 160.8 km.

5.3 3-D modelling parameters and initial models

The 3-D model size represents the number of unknowns in the forward modelling problem. If the inverse problem was to be solved in the model-space this would present a huge computational problem. In the given data set of 97 stations at 30 periods and 4 impedance responses, the problem reduces to N=97 x 30 x 4 equal to 11,640 which can be solved with achievable computational cost and memory done by data-space 3-D inversion. The inversion program was run using a parallel processing version of the WSINV3DMT code using the Message Passing Interface (MPI) parallel computing environment. This was setup on a special machine cluster at ÍSOR running on 32 cores and 132 GB of memory to be able to deal with a big data set like this one.

A 10 Ωm homogeneous half-space initial model was used as the base models for the 3-D inversions starting at initial RMS of 11.5 and reducing to 1.5 after 15 iterations. The RMS defines the data misfit between the measured and calculated values of the off diagonal tensor elements (real and imaginary parts), weighted by the variance of the measured values.

For the initial model three runs were performed and 5 iterations were allowed for each run. After every run the inversion was restarted with the model that gave the best fit as the initial model for the successive runs. Through these step-runs the inversion gradually relaxes the limitation of the prior model, until the data fit can no longer be improved. This is achieved by regularization where a reference (prior) model is used to constrain the inversion model not to deviate too much from the prior model. Each iteration took 27 hours, yielding a total computing time of 405 hours for 15 iterations. Most of the CPU time is spent in constructing the sensitivity matrix for solving inverse problems.

5.4 3-D inversion results

This section describes 3-D inversion results derived using the smoothed 10 Ωm homogeneous half-space initial model. Ordinarily the 3-D program assumes flat surface, but as mentioned earlier the MT data were static shift corrected prior to the inversion and this correction considerably removes topographic effects in the data. The resistivity models resulting from the inversion were elevation corrected, and results are presented as smoothed iso-resistivity maps (Figure 4c and 5c) and cross-sections (Figure 6c and 7c).

5.5 Discussion of 3-D inversion results

The 3-D MT inversion of the off-diagonal impedance tensor for the 97 MT sites and 30 periods revealed the main parts of the subsurface resistivity structures at the Silali geothermal field. The resistivity models revealed a typical resistivity structure for a high-temperature geothermal field as found elsewhere, i.e. a low-resistivity cap underlain by a resistive core which presumably is related to the geothermal reservoir (Eysteinsson et al., 1994; Árnason et al., 2000).

The low-resistivity anomaly observed at shallow depth particularly around the caldera and to the south of the caldera is attributed to low temperature alteration minerals. Underlain high resistivity is related to the change in alteration minerals to higher temperature mineralogy within the caldera spreading to south of the caldera. At depth of about 6 km a conductive segment dominates; this deep low-resistivity region could be associated with presence of partial melt which has been interpreted as the heat source for the geothermal system in this field. It should however be noted that the resolution of MT data at long period may not be trusted due to noise, this therefore underscores the importance of collecting good data particularly at long periods. Results from the above models show that resistivity structure up to a depth of 6 km is stable but below that the models may not be entirely correct.

6. COMPARISON OF 1-D, 2-D AND 3-D RESULTS

Results for two profiles will be compared for the 1-D, 2-D and 3-D inversion of MT data. Both 1-D and 3-D are elevation-corrected but 2-D is not. From the evaluation of the 3-modes of 2-D inversion, TM-mode result are preferred to be compared with both 1-D and 3-D models.

The 1-D, 2-D and 3-D vertical resistivity cross-sections of Profile EW10_4 (for location see Figure 3) are shown in Figure 4a, 4b and 4c). All the three resistivity cross-sections generally show a three layer resistivity structure down to depth of 6 km, with a high resistivity surface layer (> 100 Ωm) underlain by a low resistivity layer (< 10 Ωm) and a third high resistivity zone (> 70 Ωm). The deeper basal layer differs somewhat with 1-D model smearing low resistivity across the entire section rising to shallow depth at the western-most end of the profile and at the eastern edge of the caldera below site slmt172. On the other hand the 2-D profile shows low resistivity on the western half of the profile rising to shallow depths on both sides of the caldera. The 3-D model shows low resistivity at depth of 6 km b.s.l beneath the caldera with a fairly low resistivity elongation towards the surface. In all the models there is a low resistivity linear structure between the high resistivity anomaly in the intermediate depths. It should be noted that the 3-D model reveals the resistivity structure reliably well particularly the high resistivity zone where the two anomalies are clearly resolved.

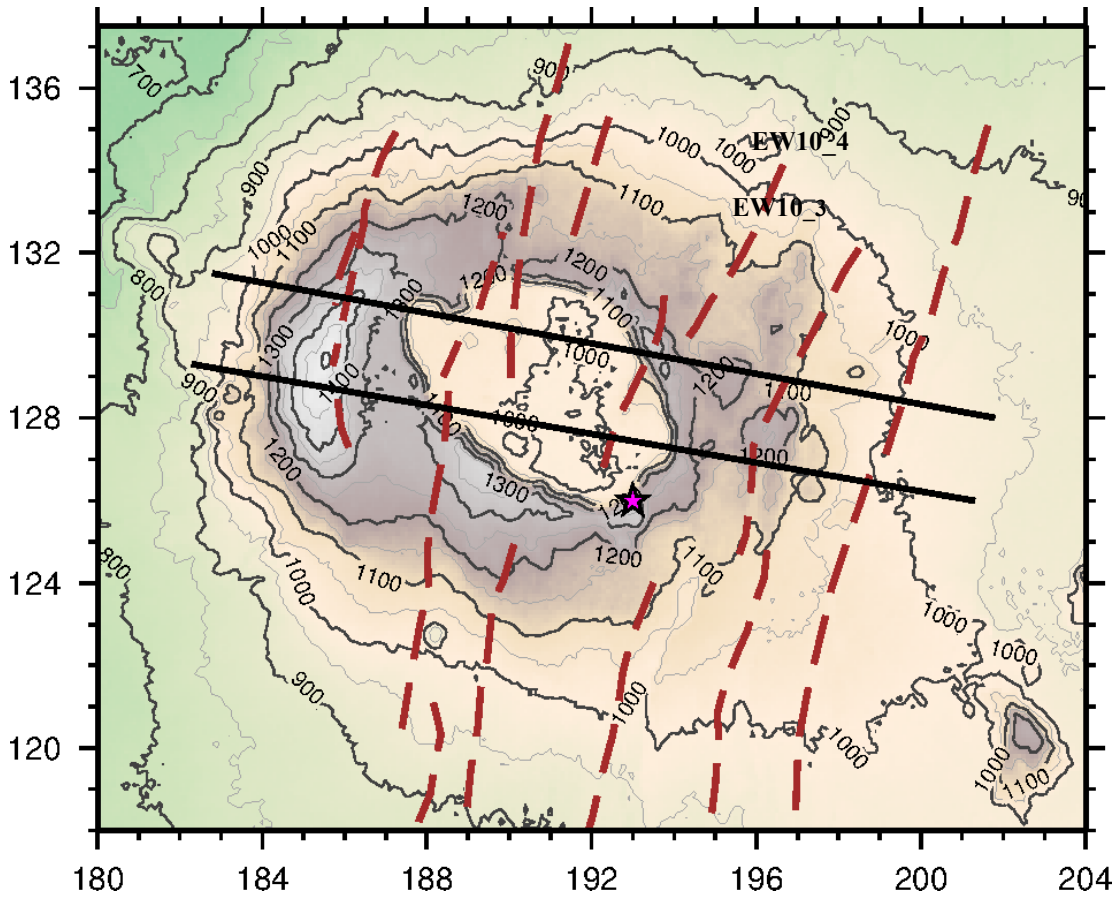

Figure 3: Location map showing cross-sections through the study area

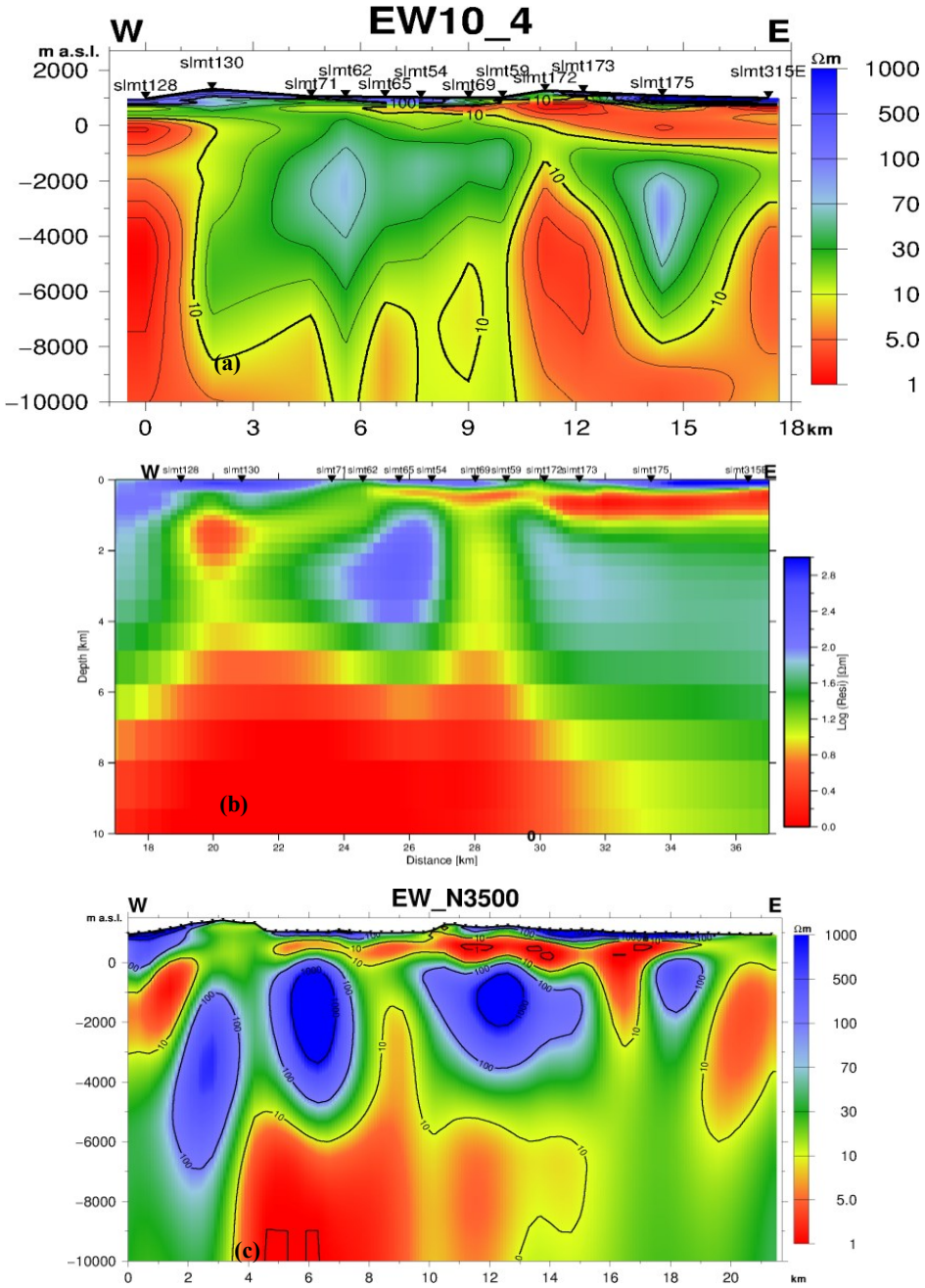

Figure 4: Comparison of 1-D, 2-D and 3-D vertical resistivity cross-sections for profile EW10_4: (a) from joint 1-D inversion of TEM and determinant MT data. (b) 2-D inversion of TM-mode and MT data (c) 3-D model at EW_N3500

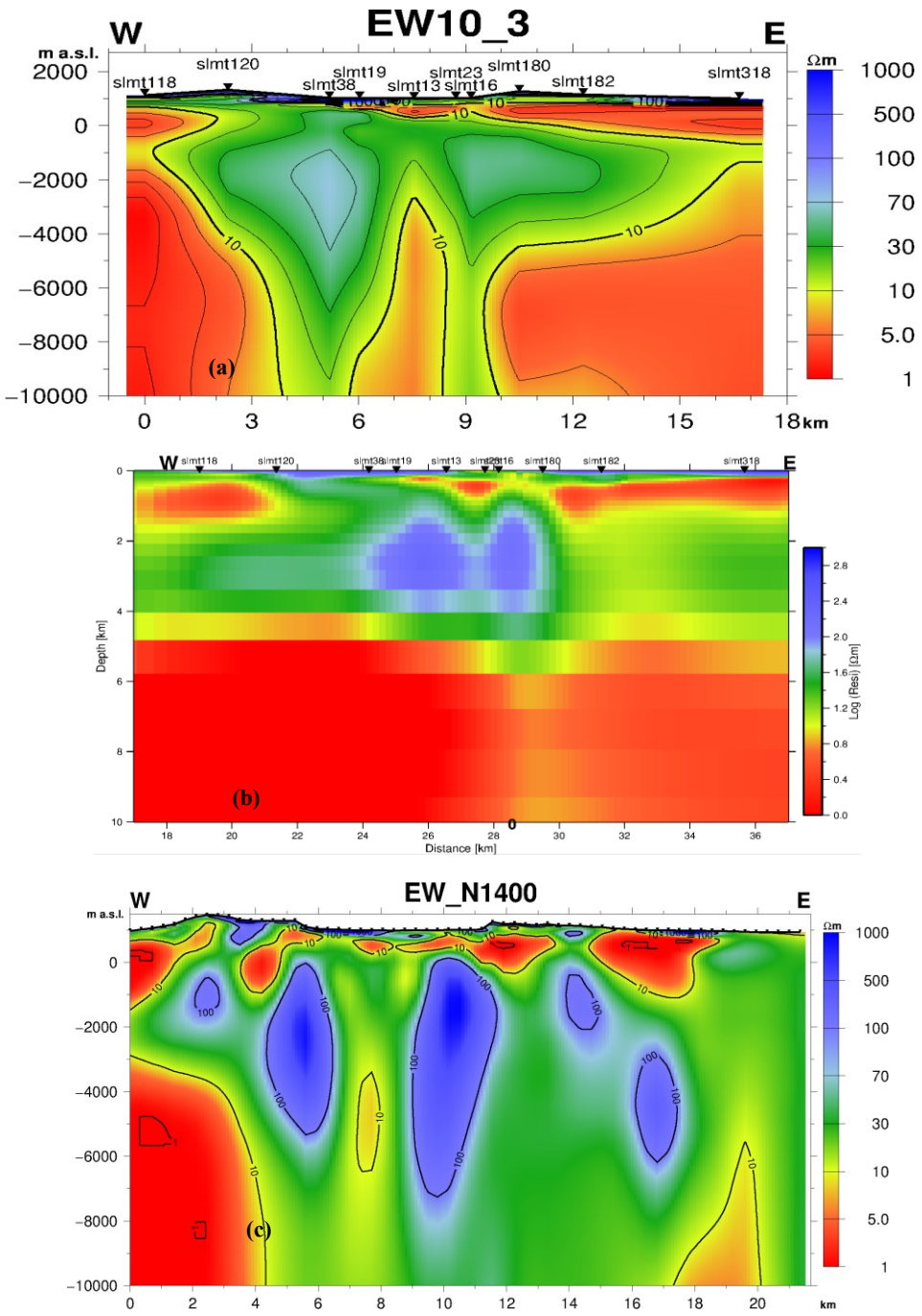

Figure 5: Comparison of 1-D, 2-D and 3-D vertical resistivity cross-sections for Profile EW10_3: (a) from joint 1-D inversion of TEM and determinant MT data. (b) 2-D inversion of TM mode MT data. (c) 3-D model at EW_N1400

Similarly resistivity structure for profile EW10_3 (for location see Figure 3) is compared in Figure 5. Likewise this profile shows a resistivity structure with a top high resistivity underlain by a low resistivity second layer followed by a higher resistivity structure. However the 3-D model has better resolved resistivity geometries both at the shallow low resistivity and the underlying high resistivity core. Of special significance are the two high resistivity anomalies separated by a lower resistivity linear structure below the caldera. At depth of 5 km b.s.l both 1-D and 2-D models present a deeper low resistivity smeared all across the entire profile. The 3-D model presents a localized deeper low resistivity beneath the caldera and extending to the west of the caldera. From this comparison it seems reasonable to conclude that the anomalies revealed are real.

The next section compares iso-resistivity maps of 1-D and 3-D developed using Linux program with 2-D maps from WinGlink program. 2-D cross-section shown above are made using REBOCC. It should be noted that colour scales for 2-D WinGlink maps differ from those of 1-D and 3-D model maps. On the WinGlink maps the caldera structure and the faults are marked by brown and black symbols respectively whereas on the other maps faults are marked by brown broken lines.

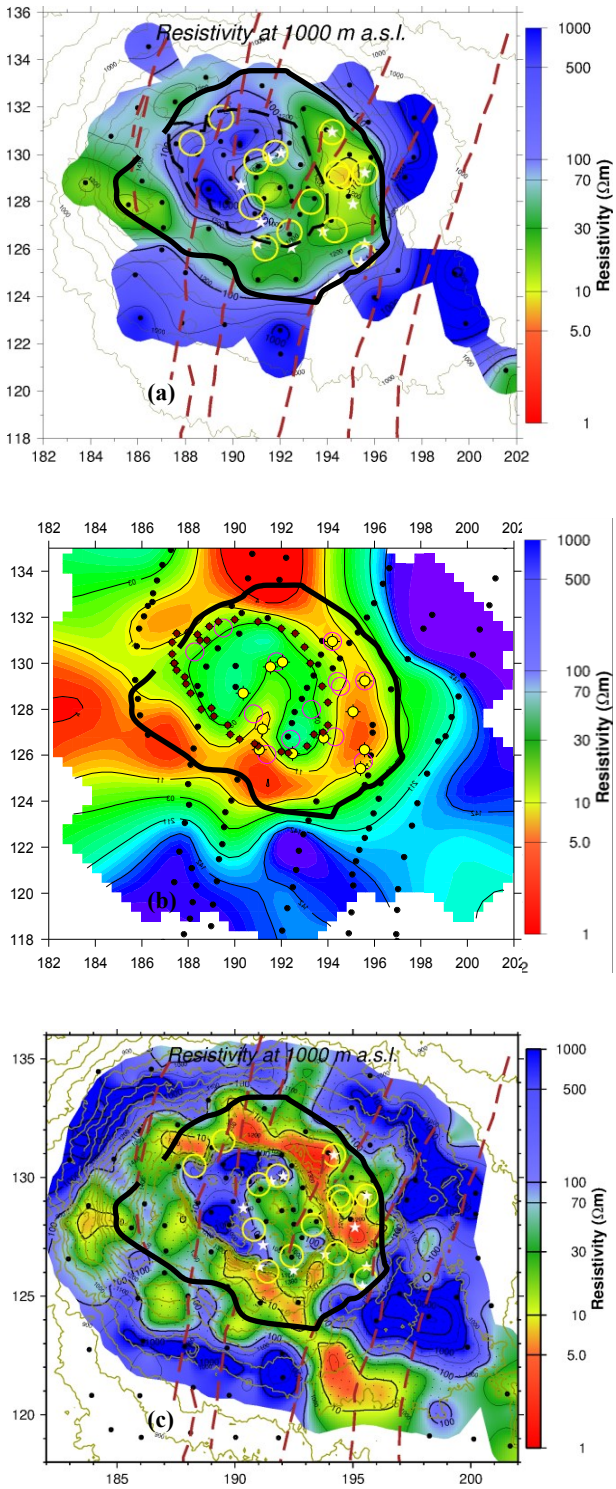

Figure 6: Comparison of 1-D, 2-D and 3-D horizontal resistivity map at 1000 m a.s.l (a) joint 1-D inversion of TEM and determinant MT data. (b) 2-D resistivity map from WinGlink. (c) 3-D resistivity map from 10 ohm-m initial model. Black line marks low resistivity boundary

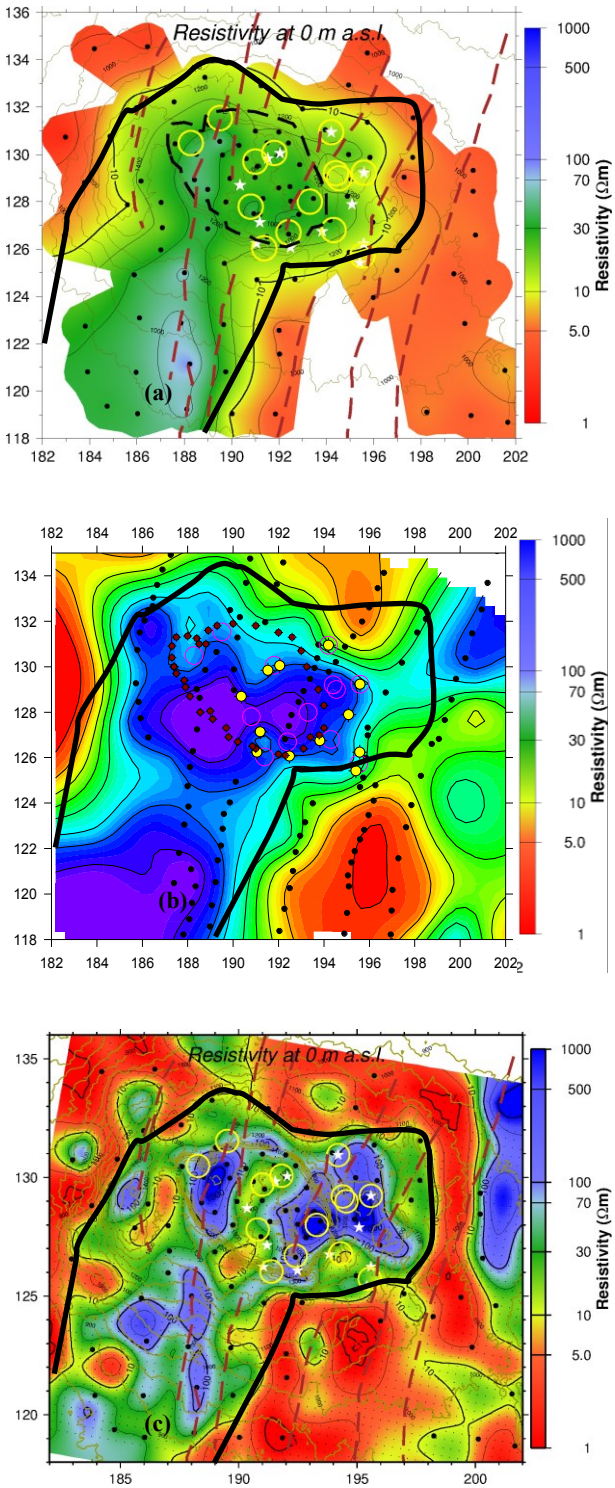

Figure 7: Comparison of 1-D, 2-D and 3-D horizontal resistivity map at sea level (a) joint 1-D inversion of TEM and determinant MT data. (b) 2-D resistivity map from WinGlink. (c) 3-D resistivity map from 10 ohm-m initial model. Black line marks high resistivity boundary.

Figure 6 shows resistivity at 1000 m a.s.l for 1-D, 2-D WinGlink and 3-D models respectively. For all the three models there is a striking correlation between the low resistivity which has been attributed to the low temperature mineral alteration and the surface manifestations at shallow depth encircling the caldera. Elsewhere a high resistivity is seen on the outer margins all around the low resistivity. Similarly Figure 7 shows resistivity at sea level with a generally high resistivity trending in a NE-SW direction from the caldera to the extreme SW end. This high resistivity zone, maps high resistivity core of the geothermal system in this field. 1-D and 2-D models smear the resistivity indiscriminately while 3-D models seems to sharpen the resistivity structure much better as seen in Figure 7c showing the two high resistivity anomalies inside the caldera.

6.1 Discussion of 1-D, 2-D and 3-D comparison

The 1-D and 2-D inversion of MT data on the two profiles (Figures 4 and 5) show three main resistivity structures down to a depth of 6 km. A high resistivity surface layer associated with fresh basaltic lava, a very low resistivity second layer (< 10 Ωm) of variable thickness was observed along the vertical cross-sections. The conductive layer is presumably associated with smectite and

mixed layer clay alteration. A high resistivity (> 70 Ωm) is observed underlying the conductive layer along the cross-sections, more resolved in the 3-D model both for Figure 4c and 5c. The high resistivity could be related to high-temperature alteration (chlorite-epidote alteration zone) down to a depth of about 4 km. The 3-D inversion revealed a more resolved deeper conductive structure than the 1-D and 2-D inversion models. The deep conductive body is presumably associated with the heat source of the geothermal system. Generally 1-D models give a rough picture, 2-D models can be difficult to resolve but 3-D resistivity models sharpen the resistivity structure.

It should however be noted that due to noise in the data at long period the results from 1-D, 2-D and 3-D differ widely and may not resolve the anomalies deeper than 6 km. This is because the noisy portion of the data can be fitted by different models. Therefore the depth of resolution is limited to 6 km.

In conclusion, it must always be remembered that in the real earth there are no such components as 2-D anomalies, all anomalies are 3-dimensional. Again since two-dimensional (2-D) interpretations frequently cannot explain important features present in field data sets from geologically complex regions, then it is inevitable that 3-D inversion has to be carried out. Often a 2-D inversion is undertaken of data that exhibit weak 3-D effects because of the inadequacy of spatial coverage (only a single profile of data rather than a grid) or because of the complexity of 3-D modelling. 2-D techniques applied to 3-D data are merely indicative and can be misleading if interpreted without consideration.

7. CONCLUSSION

A multi-dimensional interpretation of Electromagnetic data was performed for the Silali area, where 102 MT soundings have been inverted using the 1-D joint inversion of determinant MT and TEM and a 3-D inversion of the off-diagonal impedance tensor elements for 97 MT surroundings.

The objective of this study was two fold: To compare different approaches of interpreting Electromagnetic data (1-D, 2-D and 3-D) by testing the robustness of the models to recover resistivity structure and study the resistivity structure of Silali in order to infer presence of geothermal systems.

Comparison of different inversion approaches show that 1-D and 3-D inversion results are comparable, such that 1-D inversion reproduces the main resistivity structures but smears them out while the 3-D inversion sharpens the picture considerably. 2-D results are generally questionable since different modes from the same data reproduce different results.

Generally the resistivity structure of the Silali area present four resistivity segments: A surface high resistivity zone of unaltered formations, a second low-resistivity anomaly observed at shallow depth particularly around the caldera and to the south of the caldera is attributed to low temperature alteration minerals. Underlain high resistivity is related to the change in alteration minerals to higher temperature mineralogy within the caldera spreading to south of the caldera. At depth of about 6 km a conductive segment dominates; this deep low-resistivity region could be associated with presence of partial melt which has been interpreted as the heat source for the geothermal system in this field.

REFERENCES

Árnason, K., R. Karlsdóttir, H. Eysteinsson, Ó.G. Flóvenz, and S.Th. Gudlaugsson, 2000: The resistivity structure of high-temperature geothermal systems in Iceland. Proceedings of the World Geothermal Congress 2000, Kyushu-Tohoku, Japan, 923-928.

Árnason, K., 2008: The Magneto-telluric static shift problem. Iceland GeoSurvey - ISOR, report, ISOR-08088, 17 pp.

Eysteinsson, H., K. Árnason, Ó.G. Flóvenz, 1994: Resistivity methods in geothermal prospecting in Iceland. Surv. Geophy. 15, 263–275.

Eysteinsson, H., 1998: TEMMAP and TEMCROSS plotting programs. Iceland GeoSurvey - ÍSOR, Unpublished programs and manuals.

Siripunvaraporn, W., G. Egbert, Y. Lenbury, M. Uyeshima, 2005: Three-dimensional Magnetotelluric inversion: data-space method. Phys Earth Plan Int. 150:3–14.

Sternberg, B.K., J.C. Washburne, and L. Pellerin, 1988: Correction for the static shift in magnetotellurics using transient electromagnetic soundings. Geophysics, 53, 1459-1468.

Wannamaker, P. E., 1991. Advances in three-dimensional magnetotelluric modelling using integral equations, Geophysics, 56, 1716–1728.